9-1-2017

Xenopus pitx3 target genes lhx1 and xnr5 are identified using a novel three-fluor flow cytometry–based analysis of promoter activation and repression

Lara Nicole Hooker
Validation Technologies, Inc, San Diego, California

Cristine Smoczer
Biochemistry and Genetics, University of Detroit Mercy School of Dentistry, Detroit, Michigan

Samuel Abbott
Biological Sciences, University of Windsor, Windsor, Ontario, Canada

Mohamed Fakhereddin
Biological Sciences, University of Windsor, Windsor, Ontario, Canada

John W. Hudson
Biological Sciences, University of Windsor, Windsor, Ontario, Canada

See next page for additional authors

Developmental Dynamics

Xenopus pitx3 target genes *lhx1* and *xnr5* are identified using a novel three-fluor flow cytometry-based analysis of promoter activation and repression.

Journal:	*Developmental Dynamics*
Manuscript ID	DVDY-16-0136.R2
Wiley - Manuscript type:	Research Article
Date Submitted by the Author:	n/a
Complete List of Authors:	Hooker, Lara; Validation Technologies, Inc. Smoczer, Cristine; University of Detroit Mercy School of Dentistry Abbott, Samuel; University of Windsor, Biological Sciences Fakhereddin, Mohamad; University of Windsor, Biological Sciences Hudson, John; University of Windsor, Biological Sciences Crawford, Michael; University of Windsor, Biological Sciences
Keywords:	flow cytometry, gene regulation, promoter analysis, Xenopus laevis, embryogenesis, laterality, pitx3, lhx1, xnr5, tyrosine hydroxlase

Xenopus pitx3 target genes lhx1 and xnr5 are identified using a novel three-fluor flow cytometry-based analysis of promoter activation and repression.

Lara N. Hooker[1], Cristine Smoczer[2], Samuel Abbott[3], Mohamad Fakhereddin[3], John W. Hudson[3], Michael J. Crawford[3*]

[1]Validation Technologies, Inc., 10815 Rancho Bernardo Rd, San Diego, CA 92127, USA

[2]Biochemistry and Genetics, University of Detroit Mercy School of Dentistry, 2700 Martin Luther King Jr Blvd, Detroit, MI 48208, USA

[3]Biological Sciences, University of Windsor, 401 Sunset Ave. Windsor, ON. N9B 3P4, Canada

*Author for correspondence: mcrawfo@uwindsor.ca Tel: (519) 253 3000 (x 2721)

Keywords: flow cytometry, gene regulation, promoter analysis, Xenopus laevis, embryogenesis, laterality, pitx3, lhx1, xnr5, tyrosine hydroxyase

Grant Sponsor: Natural Sciences and Engineering Research Council of CANADA Grant number 203459 to MJC and 05947 to JWH

ABSTRACT

Background: Pitx3 plays a well understood role in directing development of lens, muscle fiber, and dopaminergic neurons, however in *Xenopus laevis*, it may also play a role in early gastrulation and somitogenesis. Potential downstream targets of pitx3 possess multiple binding motifs that would not be readily accessible by conventional promoter analysis.

Results: We isolated and characterized pitx3 target genes *lhx1* and *xnr5* using a novel three-fluor flow cytometry tool that was designed to dissect promoters with multiple binding sites for the same transcription factor. This approach was calibrated using a known pitx3 target gene, *tyrosine hydroxylase*.

Conclusions: We demonstrate how flow cytometry can be used to detect gene regulatory changes with exquisite precision on a cell-by-cell basis, and establish that in HEK293 cells, pitx3 directly activates *lhx1* and represses *xnr5*.

INTRODUCTION

The mammalian *Pitx* gene family belongs to the OAR (*Otx, Arx, Rax*) subgroup of *paired*-like transcription factors (TF). One member of this family, *Pitx3*, is expressed in the *substantia nigra compacta* where it is responsible for the maturation and final differentiation of mesencephalic dopaminergic neurons and also for the subsequent regulation of the dopamine rate-limiting enzyme, tyrosine hydroxylase (van den Munckhof et al., 2003; Smidt et al., 2004; Maxwell et al., 2005). *Pitx3* also expresses in developing somites, lens placode, and in forming lens pit (Smidt et al., 1997; Semina et al., 1998; Smidt et al., 2004). In mice, *Pitx3* is the causative locus for *aphakia*, a recessive deletion mutant resulting in small eyes that lack lenses (Semina et al., 1998). Similar mutant phenotypes are seen in humans (Semina et al., 1998; van den Munckhof et al., 2003). During myogenesis, both *Pitx2* and *Pitx3* participate in the differentiation of skeletal muscles (Coulon et al., 2007; L'Honore et al., 2007).

While *Xenopus laevis pitx3* plays a similar role during eye development, it additionally expresses during gastrulation as well as later the in pre-somitic mesoderm, lateral plate mesoderm, differentiating somites, craniofacial regions, and in looping heart and gut (Pommereit et al., 2001; Khosrowshahian et al., 2005; Smoczer et al., 2013). In contrast to mammals, *Xenopus pitx3* also affects laterality (left-right organ asymmetry) and somitogenesis (Khosrowshahian et al., 2005; Smoczer et al., 2013). Remarkably, these latter phenotypes are elicited by both gain of function as well as by morpholino-mediated translational knockdown (Smoczer et al., 2013). We decided to identify some of the *pitx3* target genes that might mediate both eye as well as novel phenotypes.

We performed a microarray-based search for potential downstream target genes and defined a preliminary list of potential target genes based upon near-coincident timing and domain of expression. This list initially comprised roughly 80 candidates, however it was refined using RT-PCR followed by riboprobe *in situ* hybridization to those most likely to perform as legitimate *pitx3* targets (Hooker et al., 2012). We then further selected a subset of genes that possessed pitx3-binding motifs in their respective promoter/enhancer regions (based upon elements identified in *X. laevis* or *tropicalis* sequences and conserved in fish or mammalian species). Two likely play a conserved role in eye development and possess multiple pitx3 binding motifs (*lhx1* and *xnr5*).

A drawback of most reporter assays is that reporter gene expression is assayed in a heterologous population of transfected and untransfected cells, where estimation of the ratio between populations is difficult: lysates homogenize and average cellular results of transcription factor activity, so it is hard to assess quantitative effects on a per-cell-basis. To circumvent this shortcoming, other studies have deployed a dual luciferase reporter assay where the reporter vector and another bioluminescent gene driven by a constitutive promoter is introduced to serve as control for transfection efficiency (Stables et al., 1999). Although widely employed, this approach relies upon the presumption that both vectors have identical or at least similar transfection properties. Our putative targets have multiple candidate response elements that would not be easily dissected using either approach.

To address these shortcomings, we devised a novel flow cytometry-based protocol that works exquisitely well to link transcription factor input to promoter reporter output on a cell-by-cell basis. By counting only those cells that are co-transfected, we can

estimate how promoters work even if responses are non-linear. The system relies upon co-transfection of two plasmids: one comprises a CMV-*eGFP* IRES unit that is bicistronically linked to the transcription factor – in this case *Pitx3* (input) called *Pitx3-IRES-GFP*; the other houses CMV-*HcRed1* (target availability) orientated in opposition to a target-promoter driven reporter, *CMV-HcRed/target promoter-DsRed* (output). Since only those cells that are co-transfected are analyzed, differences in transfection efficiency between treatments are rendered irrelevant. In addition, a ratio between the two transfected plasmids can be generated for each cell: there is good quantitative data to indicate how much transcription factor is being expressed, how much target is available, and how much that target is activated/repressed. As proof of principle, we calibrated our system against a well-characterized promoter, murine *tyrosine hydroxylase* (*Th*). We have defined the range of transfection parameters within which the system reports with fidelity and in linear fashion – in other words, the range at which GFP accumulation and fluorescence is proportionate to pitx3 detectable on Western blots.

Based upon our preliminary slate of putative signaling targets, our suspicion is that pitx3 plays a heretofore uncharacterized role during gastrulation by regulating *lhx1* and *xnr5*, and in a manner that explains why both *pitx3* under- and over-expression leads to similar dorsal axis phenotypes.

RESULTS

Construction of the expression and reporter vectors. Our system relies on two participating plasmids. The first is a bicistronic expression vector, *Pitx3-IRES-GFP*, which harbors the transcription factor *pitx3* and *GFP* (Fig.1), and that simultaneously

produces two proteins from a single mRNA transcript (Trouet et al., 1997). A corresponding pitx3 homeodomain-binding mutant was constructed by inserting a mutated form of *pitx3* as the first coding sequence of the bicistronic unit. The L99P amino acid substitution within the DNA-binding homeodomain was modeled after one described for another *paired*-like homeodomain *mixl1,* shown to hinder binding of the transcription factor to its target DNA sequences and to act as a dominant negative inhibitor (Mead et al., 1996). This mutant, called *Pitx3^{mutHD}-IRES-GFP*, was tested to see if it served similarly in our studies. The second vector harbors the promoter reporter and a transfection calibration fluor (Fig.1B). Depending upon the promoter analysed, these vectors were called *CMV-HcRed/Th-DsRed* (to assess a previously characterized *Tyrosine hydroxylase* promoter activity), *CMV-HcRed/lhx1-DsRed* (to assess *X. laevis lhx1 promoter* activity), or *CMV-HcRed/xnr5-DsRed* (to assess *X. laevis xnr5 promoter* activity). Deletion mutants, *CMV-HcRed/th$^{mut-350}$-DsRed, CMV-HcRed/lhx1$^{mut-709}$-DsRed, or CMV-HcRed/xnr5^{mut-94}-DsRed* were also generated for promoters to serve as specificity controls by prohibiting pitx3 binding: *th* mutant (-350bp from ATG: TAATCC to TAccCC), *xnr5* mutant (-94bp from ATG: TAAGCT to TcgaCT), and *lhx1* mutant (-709bp from ATG: TAATGG to TccaTGG).

Calibration of pitx3 relative to eGFP in cells transfected with the bicistronic expression plasmid. In order to ensure the reliability and the linear operating range of the system, we established the correlation between the levels of the two proteins produced by the bicistronic vector. We assessed the ratio of eGFP and pitx3 in two separate experiments: one to determine plasmid concentration dependence, and a second to ensure that the ratio remains constant over time.

HEK293 cells were transiently transfected with four different dilutions of *Pitx3-IRES-GFP* and assessed by Western blotting. This series allowed the maximum number of dilutions resulting in observable protein by pitx3 antibody. The protein band intensities for eGFP and pitx3 proteins were compared and linear regression analysis reveals a strong and consistent correlation between the two proteins across all concentrations (Fig.2).

Moreover, at these transfection concentrations both proteins have parallel accumulation rates across time. A set amount of *Pitx3-IRES-GFP* was transfected into HEK293 cells and cell lysates were collected at 24 hours, 36 hours and 48 hours. The ratio between the pitx3 and GFP proteins levels is constant, with no statistically significant differences between time-points (Fig.2B). However the ratio between pitx3 and GFP protein levels at the 48 hour time-point could suggest unequal degradation/lifespan rates for the two proteins.

GFP protein concentrations correlate with GFP fluorescence in transfected cells. The total fluorescence for each population of transfected cells in the dilution and time-point experiments was plotted relative to the GFP protein band intensity analyzed by immunoblotting. This determines if changes in GFP fluorescence are accurately reflecting changes observed at the protein level. In triplicate experiments, regression analysis revealed a very strong correlation between GFP protein and fluorescence irrespective of the amount of vector that was transfected or post-transfection time of analysis (Fig.3).

Flow cytometry protocol for the three-fluor reporter assay. For acquisition of accurate signals from each fluorescent protein, we developed an optimal flow cytometry

protocol to separate the three fluors into discrete channels with minimal spectral overlap. The forward versus side scatter data is used to restrict the selection solely to viable cells. Each fluor is analyzed in a separate control and the appropriate voltage necessary for optimal fluor excitation is established (see Experimental Procedures Table 1). As controls to set-up experimental parameters, we used cells transfected separately with each of the vectors *IRES-GFP, CMV-HcRed, CMV-DsRed*, as well as with a combination of the *IRES-GFP* and *HcRED1* empty vectors. The GFP signal is collected in channel FL1, the HcRED1 in channel FL5 (Fig.4, A and B). DsRed signal was collected in channel FL2. This allows us to gate on each fluor in order to minimize background fluorescence and to establish proper compensation for each signal to reduce spillover into other channels. These controls were run prior to each individual experiment. From the cells that were co-transfected with both *GFP* and *HcRED1* control vectors, we collected 10^4 cells in the gate with active signal for both fluors (Figure 4C), and this co-expressing population was plotted on a FL2 histogram to collect the total background DsRed fluorescence that was subsequently subtracted from each experimental data set (Figure 4D).

The final step for each reporter experiment was to assess the degree to which incremental increases of the transcription factor affected the tested promoter. In some special cases, binding of transcription factor to one site facilitates subsequent binding to others. This is called co-operativity (Beachy et al., 1988). The cells expressing all three fluors were represented on a dot-plot with the DsRed as ratio of HcRed fluorescence: this accounted for the amount of reporter plasmid transfected (reporter output) correlated to GFP fluorescence (transcription factor input). A linear regression of the analysis permits us to assess the slope of activation or repression.

Calibration utilizing the previously characterized pitx3 and *Tyrosine hydroxylase* interaction. To test our new technique, we used the well-studied activity of pitx3 upon the murine *Tyrosine hydroxylase (Th)* promoter (Cazorla et al., 2000), *CMV-HcRed/Th-DsRed*. The two players in our system include the 1.5kb mouse *Th* promoter, which is sensitive via an active pitx3 binding site (Cazorla et al., 2000; Lebel et al., 2001), and the *Xenopus pitx3* coding sequence contained in plasmid *Pitx3-IRES-GFP*. The homeodomains of murine and frog Pitx3 are identical. The HEK293 cell line was used, where Pitx3 is known to act as a repressor for *Th* (Cazorla et al., 2000). This cell line is useful for have a previously demonstrated ability to respond to pitx3, however recently has been shown to possess some intrinsic confounding features: the Human Protein Atlas project, at www.proteinatlas.org (Uhlen et al., 2015), indicates that it suffers the disadvantage of expressing both pitx1 and pitx2, transcription factors that encode near-identical homeodomains. The endogenous levels of the *Th* reporter were found to be very low in this cell line and therefore the repression induced by *pitx3* was very small, although significant. Given the strong *Th* activation by cyclic AMP independent of pitx3 (Cazorla et al., 2000), we chemically activated the *Th* promoter with forskolin and thus allowed for a potentiation of pitx3 repressive activity. Using the novel reporter assay, we show that pitx3 represses *Th* output by approximately 80%, while the pitx3 homeodomain mutant, *Pitx3^{mutHD}-IRES-GFP,* leaves expression unchanged (Fig.5). Conversely, by site-directed mutagenesis we mutated the known Pitx3 binding site within the *Th* promoter (Lebel et al., 2001) and, as expected, pitx3 has no significant effect on *Th* promoter activity in the absence of the critical binding site (Fig.6).

When cells that express all three fluors are assessed, and the reporter output

(DsRed) is normalized to its availability (HcRed), a super-abundance of pitx3 (indicated by GFP) produces no extra effect: the line is flat (Fig. 7). This indicates that once the critical pitx3-binding motif is occupied, additional concentrations of pitx3, and presumably subsequent occupancy of the remaining or cyptic sites, produce no effect. In other words, it is unlikely that binding at the critical site facilitates binding at other sites: there is no indication of transcription factor co-operativity in regulation of this gene.

***lhx1* promoter tested as a novel direct target of pitx3.** The *Xenopus laevis* promoter for *lhx1*was cloned into the reporter plasmid, *CMV-HcRed/lhx1-DsRed,* and assessed for reporter activity. *Lhx1* is significantly activated by pitx3 (Fig.8) in HEK293 cells. To determine the site responsible for pitx3 binding in the targeted promoter, we interrogated the ENSEMBL.org database for the respective promoter sequences in *Xenopus tropicalis* and zebrafish. They were subsequently aligned using the MULAN software (Ovcharenko et al., 2005) and searched for conserved known Pitx3 binding sequences (TAAT(C/G)N) (Lebel et al., 2001). The sites that were conserved were mutated by site-directed mutagenesis and assessed for *pitx3*-inducible effects (Figures 8A and B).

When the promoter motif that binds pitx3 is mutated using plasmid *CMV-HcRed/lhx1*$^{mut\text{-}709}$*-DsRed*, pitx3 influence on the reporter activity is abolished and the DsRed output returns to basal levels. Pitx3 input and the reporter output was linear.

Conversely, *xnr5* expression appears to be repressed by pitx3 activity in HEK293 cells (Fig.9). VegT was used to activate *xnr5* that was assessed using reporter *CMV-HcRed/xnr5-DsRed*, and the pitx3 binding site that was found to have an effect resided between the TATA box and the ATG start methionine codon. When pitx3 was expressed,

fluorescence output diminished. When this binding motif was mutated (using plasmid *CMV-HcRed/xnr5^{mut-94}-DsRed)*, even in the absence of pitx3, expression of *xnr5* diminished. This effect could be duplicated by mutation of the pitx3 homeodomain (*Pitx3^{mutHD}-IRES-GFP*) to preclude activation of the wild type *xnr5* promoter.

Expression of *lhx1* is altered by *pitx3* activity (Fig.10). When the lhx1 promoter's pitx3 binding motif is impaired in tissue culture (Fig. 8), or in trangenics (compare Fig. 10A with A'), lhx1 expression is depressed. *Lhx1* would normally express in the lip at gastrulation, and this is reflected by GFP expression in "wild-type" promoter/reporter transgenics. In transgenics lacking a pitx3 binding motif in the *lhx1 promoter*, gfp expression falls. While *pitx3* morphants yield a phenotype that is less spectacular, *lhx1* expression loses its characteristic and smoothly graded expression around the gastrulation lip such that the lateral lip mesoderm expresses more lightly than ventral lip (compare B to arrows in B'). The domain of *gsc* expression (a dorsal mesoderm marker) expands (compare arrows in C and C'), however *t* (a pan mesodermal marker at this stage) diminishes slightly at the lateral lip. (compare D and D').

In the case of *xnr5*, the 20% diminiution of activity seen in flow cytometry studies does not translate to visible changes to in vivo expression. In *pitx3* morphants, the expression of *xnr5* downstream effectors in the left-expressing laterality pathway (*xnr1, lefty*, and *pitx2*) are reduced or abolished, leading to morphological randomization of laterality (compare control injected Fig. 10 E, F, and G with E', F', and G').

DISCUSSION

We have developed a novel and innovative reporter technique and tested its efficacy using a known pitx3 interaction before utilizing the assay to assess new potential targets for this transcription factor. An IRES plasmid could introduce a few variables since the two separately translated proteins might be post-translationally modified and degrade or clear at different rates. Before making this plasmid a component of our

system, we ensured that the detected GFP fluorescence accurately reflects the titers of pitx3 protein present in cells by demonstrating that the ratio between pitx3 and GFP is a reliable parameter within the concentration ranges deployed and that it was independent of concentration and time of analysis (Figures 2 and 3).

The novelty of the technique is enhanced by the introduction of a reporter plasmid which itself contains a constitutively driven fluorescent protein, HcRed1, to serve as an indicator for transfection efficiency and target availability. Flow cytometry permits us to analyze only the cells that are co-transfected: the analysis delivers quantitative data regarding transcription factor concentrations (input), candidate promoter plasmid availability, and candidate promoter reporter activity (output) (Figure 4).

To calibrate the specificity and sensitivity of the newly developed method, we tested the interaction between pitx3 and the murine *Tyrosine hydoxylase* promoter. Pitx3 operates by association with other co-factors such as MTA1 and Nurr1 to ensure efficient regulation of *tyrosine hydroxylase* (*TH)* (Cazorla et al., 2000; Reddy et al., 2011; Volpicelli et al., 2012), and therefore the outcome of this interaction is highly dependent upon the cellular context (Messmer et al., 2007; Medina-Martinez et al., 2009). We chose the HEK293 cells line where the interaction has been previously analyzed by luciferase assay and where murine Pitx3 is known to inhibit *Th* transcription (Cazorla et al., 2000). In order to increase the basal activity of the *Th* promoter we used forskolin to boost the levels of cAMP, which is known to bind to the cAMP-response element (CRE) on the *Th* promoter and induce its activation (Cazorla et al., 2000). Our data confirms a 70-80% repression by *Xenopus* pitx3 in both basal and forskolin-activated states; levels identical to those observed by luciferase assay (Cazorla et al., 2000) (Figure 5A). Mutating a site

in the *Th* promoter known to be responsible for pitx3 binding (Lebel et al., 2001), we were able to also confirm the specificity of our technique by prohibiting pitx3 interaction with the *Th* promoter (Figure 5B). Finally, we further confirmed specificity by testing a pitx3 homeodomain mutant to show that a binding-defective protein cannot induce transcriptional repression in the target gene. Flow cytometry is both expensive and time consuming, and does not translate well to dual-luciferase style promoter assays. We experimented with mimicking a dual luciferase assay using flow cytometry and found the samples to show unusefully high standard deviations (data not shown). We surmise this is because the laser excitation of fluors in cells extends the shoulders of excitation distribution curves, the experiment uncouples direct quantification of target availability and transcription factor input from reporter output, and this, combined with a smaller replicate size (3 versus 6 or more), leads to much higher variation. The advantage of the three fluor system is does not require an inferred plasmid transfection efficiency based upon an unlinked reporter, but the fluors can instead offer the possibility to gate quantification solely to the cell sub-populations that carry transcription factor and target, as that express a promoter-reporter. Dual luciferase assays are simpler, faster, and cheaper, and three fluor flow cytometry-based methods should only be considered when a promoter possesses more than a handful of likely binding motifs for a given factor.

Our two candidate pitx3 target genes are interesting insofar as they are known to play a role during gastrulation, early dorsal axis development, as well as later during eye development. Previous work has indicated that *pitx3* expresses in fish hypoblast (Dutta et al., 2005), and in *Xenopus* pre-gastrula (RT-PCR), and dorsal mesoderm (in situ) (Khosrowshahian et al., 2005; Smoczer et al., 2013). *Lhx1* is a *LIM*-class homeodomain

transcription factor that is expressed in several waves, the first of which is in Spemann's organizer where it expresses in the involuting mesodermal cells (Taira et al., 1992; Hukriede et al., 2003). A second wave of expression occurs during tailbud stages in the pronephric kidney and fore-, mid-, and hindbrain (Taira et al., 1992; Cirio et al., 2011). *Lhx1* is extremely important for anterior development of the embryo: *Lhx1* mutant mice present a headless phenotype (Shawlot and Behringer, 1995). *Lhx1* directly targets and activates *gsc* expression and may be responsible for maintained *gsc* expression during late gastrulation within the prechordal plate (Mochizuki et al., 2000). In chicks, *Lhx1* plays a critical role in retinal development (Kawaue et al., 2012; Inoue et al., 2013). In the present study, *Xenopus lhx1* expression is identified as a *pitx3* target (assessed by microarray, *in situ* hybridization), expression patterns overlap with *pitx3*, and the gene contains multiple putative binding sites in its enhancer/promoter (Hooker et al., 2012). Curiously, although pitx3 unambiguously activates the *lhx1* reporter in tissue culture ($p=0.004$), removal of a pitx3 binding motif alone is sufficient to repress activity under circumstances where no pitx3 is present. We attribute this to the documented presence of pitx1 and pitx2 in HEK 293 cells (Uhlen et al., 2015). In the absence of a binding site, these confounding factors that encode identical homeodomains cannot activate the reporter. Significanltly, when the pitx3 binding site is removed, pitx3 cannot activate lhx1 ($p=0.001$).

In embryos, knockdown of *pitx3* does not entirely diminsh *lhx1* expression: the lateral dorsal lip seems to be the sole domain affected. One of the effects of *lhx1* depletion is the disruption of protocadherin expression (Hukriede et al., 2003; Fossat et al., 2015). Either too little or too much protocadherin impairs normal rotation of

presomitic mesoderm preliminary to the formation of discrete somites (Kim et al., 2000). Therefore, *pitx3*-induced disruption of *protocadherin* via *lhx* perturbation would explain why *pitx3* over- or under-expression leads to identical segmentation phenotypes in *Xenopus* (Smoczer et al., 2013). Mutation of the pitx3 binding motif is sufficient to depress *lhx1* promoter activity in vitro and the effect in transgenic embryos is more profound- expression appears to be almost completely impaired. By contrast, *pitx3* knockdown only affects lateral mesoderm expression. We speculate that enhancers remote from the 3.8 kb *lhx1* sequence tested must play a role in moderating pitx3-induced effects in vivo.

One perplexing element of *xnr5* analysis was that mutation of the promoter motif critical to pitx-induced repression resulted in down-regulation even in the absence of pitx3. The site sits between the TATA box and ATG initiation codon. There are three possibilities. First, the binding motif could serve as a promiscuous site for other homeobox proteins that otherwise activate *xnr5*. Pitx1 and Pitx2, already present in HEK 293 cells are obvious candidates. Second, the mutation could impede the ability of other, nearby sites to function normally. One such candidate is M-CAT binding factor, a muscle specific factor that might utilize an overlapping binding motif on the opposite strand. Last, the mutation could adversely affect local chromatin topology to impede normal transcriptional initiation. Given the identification of *xnr5* as a candidate locus by microarray; *in situ* hybridization studies following *pitx* perturbation; and repression that is reversible by mutation of the *pitx3* homeodomain in our flow cytometry study, it seems likely that the binding site is legitimate.

Vg1 and *xnr5* share responsibility for inducing mesoderm, and the onset of gastrulation requires *xnr5* activity. *Xnr5* then represses ectodermal genes via inhibition of the *wnt* pathway (Takahashi et al., 2000; Onuma et al., 2005; Luxardi et al., 2010; Tadjuidje et al., 2016). *Xnr5* can act at a distance and is autoregulatory, however it is restricted by *lefty* and *t* (Sakuma et al., 2002; Cha et al., 2006; Ohi and Wright, 2007). *T* is a pan-mesodermal marker that acts as a transcriptional activator and it is later expressed in mesodermal cells fated to become notochord after gastrulation (Smith et al., 1991; Conlon et al., 1996). *T* and *gsc* are capable of inhibiting each other in late gastrulae: they refine head and trunk organizer regions for the prechordal plate (*gsc*) and notochord (*t*) (Mangold, 1933; Artinger et al., 1997; Mochizuki et al., 2000). *Gsc* is a potential target gene of pitx3 (Hooker et al., 2012). In *pitx3*-depleted embryos, we see an interrupted pattern of *t* expression around the forming blastopore of gastrulating embryos, compared to the continuous, mesoderm-encompassing expression domain in controls (Figure 10C and H). With the *gsc*-expressing domain larger than normal in morphants, *pitx3* morphant embryos may exhibit errors in distinguishing these separate organizer regions for patterning the head and trunk. It is also possible that the diminution of both *lhx1* and *t* in the lateral dorsal lip of *pitx3* morphants is indicative of aberrant formation of the boundary separating dorsal from ventral. It would be worth assessing both of these possibilities in the future using antero-posterior and dorso-ventral probes. Finally, *xnr5* has been identified as an upstream regulator of *xnr1, lefty,* and *pitx2* (Tadjuidje et al., 2016). Our study, confirmed by in situ hybridization of the relevant downstream targets, places *pitx3* one step further up in the hierarchical control of laterality, and explains

laterality phenotypes previously reported (Khosrowshahian et al., 2005; Smoczer et al., 2013).

Making use of different fluorescent proteins spread over a wide range of excitation and emission ranges, and the powerful tool of flow cytometry, we created a new assay to evaluate the output of a reporter gene on a cell-by-cell basis. In essence, each cell harbors an individual reporter assay, producing a cumulative, extremely accurate result that is derived from a selective and homogenous population. The assay also confers the benefit of permitting analysis in cases where high transfection efficiency is not possible while simultaneously permitting the detection of very slight variations of reporter output that might not be distinguishable by conventional methods. Our technical approach for promoter analysis has revealed a role for *lhx1* and *xnr5* as downstream targets of pitx3. The relationships that we have identified and intend to study will help to clarify the evolutionary divergence in the patterns of gastrulation and somite development between amphibians and amniotes.

EXPERIMENTAL PROCEDURES

Plasmid constructs

Plasmid names, function, and application are summarized in Table 1.

Plasmid	Species Source	Functional Description	Test system
IRES-GFP	*vector*	calibration	*in vitro* HEK 293
CMV-HcRed	*vector*	calibration	*in vitro* HEK 293
CMV-DsRed	*vector*	calibration	*in vitro*

			HEK 293
pitx3*-IRES-GFP*	*Xenopus laevis*	*pitx3* ORF	*in vitro* HEK 293
pitx3*^{mutHD}-IRES-GFP*	*Xenopus laevis*	*pitx3* ORF homeodomain mutated L99P	*in vitro* HEK 293
*CMV-HcRed/**Th**-DsRed*	*Mus musculus*	*Tyrosin Hydroxylase* promoter driving DsRed	*in vitro* HEK 293
*CMV-HcRed/**lhx1**-DsRed*	*Xenopus laevis*	*lhx1* promoter driving DsRed	*in vitro* HEK 293
*CMV-HcRed/**xnr5**-DsRed*	*Xenopus laevis*	*xnr5* promoter driving DsRed	*in vitro* HEK 293
*CMV-HcRed/**Th**$^{mut-350}$-DsRed*	*Mus musculus*	*Tyrosin Hydroxylase* promoter – pitx3 biding site at -350 mutated	*in vitro* HEK 293
*CMV-HcRed/**lhx1**$^{mut-709}$-DsRed*	*Xenopus laevis*	*lhx1* promoter – pitx3 binding site at -709 mutated	*in vitro* HEK 293
*CMV-HcRed/**xnr5**$^{mut-94}$-DsRed*	*Xenopus laevis*	*xnr5* promoter – pitx3 binding site at -94 mutated	*in vitro* HEK 293
lhx1*-GFP*	*Xenopus laevis*	*lhx1* promoter driving GFP, I-Sce transgenic vector	*in vivo* transgenic *Xenopus*
lhx1*$^{mut-709}$-GFP*	*Xenopus laevis*	*lhx1* promoter pitx3 binding site at -709 mutated, I-Sce transgenic vector	*in vivo* transgenic *Xenopus*

Table 1. Summary of plasmids used, species source of functional insert, utility, and test system.

Expression plasmid (*pPitx3-IRES-GFP*). The *pitx3* coding sequence was PCR-amplified from *pBSK-pitx3* (NM_001088554) with primers harboring adaptors for *XhoI* and *EcoRI*, and cloned into the *pCI-Neo/IRES-GFP* [F64L/S65T] bicistronic vector (kindly provided by Dr. J. Eggermont). The rationale for using a bicistronic vector as

opposed to a fusion protein lies in the known intramolecular folding that occurs in the Pitx2 protein. In the absence of cofactors binding to it, the C-terminal region of the protein comes in direct contact with the N-terminus and masks the homeodomain preventing the transcriptional activation of the target genes (Amendt et al., 1999). A DNA binding mutant (BM) was produced through site-directed mutagenesis, by mutating the leucine into a proline at position 39 of the pitx3 homeodomain sequence – in the hinge region between helix II and III (L99P).

TH Reporter plasmid. The *pCS2-HcRED1* vector was generated through PCR-amplification of the *HcRED1* sequence from *pCAG-HcRED1* (Add Gene collection) and subsequent ligation into the *XhoI*/*ClaI* sites of *pCS2-*. The reporter cassette was built by PCR-amplifying 1.5kb upstream from ATG of the murine *tyrosine hydroxylase* promoter from the *3805-4 mTH* vector (kind gift from Dr. R. Palmiter). The amplicon was sub-cloned into the *EcoRI/SmaI* restriction sites of *pDsRED*-express-N1 (Clontech). Subsequently the *mTH-DsRed*-express reporter cassette was PCR-amplified out of the previous vector and cloned in opposite orientation to *HcRED1* using the *SacII/KpnI* restriction sites of a second multiple cloning site of *pCS2-HcRED1*. This produced the dual-fluor vector *pHcRED1/mTH-DsRed*. For a control, a critical Pitx3-binding motif (underlined) in the *TH* promoter (Lebel et al., 2001) was mutated (small case) to form a *KpnI* site (bold) (CTTGGGTAATCCAGC → CTTG**GGTAcc**CCAGC).

Lhx1 promoter and mutant (*pHcRed/lhx1-DsRed*). The *lhx1* reporter plasmid was created by PCR-amplification of the *lhx1* promoter from plasmid *xLim1:luciferase Ex-1:A* (kind gift from Dr. Igor Dawid) and cloned into *EcoRI* and *BamHI* sites of *pDsRED*-express-N1. The *lhx1:DsRED* transcription cassette was again PCR-amplified and blunt

cloned in reverse direction into the *PvuII* site of *pCS2-HcRED1*. An *lhx1* mutant promoter was generated via site-directed mutagenesis utilizing primers CCC TGG TAA ACC ATg gAG CAC CCC GGC AGG and CCT GCC GGG GTG CTc caT GGT TTA CCA GGG. to introduce a novel NcoI site (TAATGG mutated to TccaTGG).

Lhx1 promoter-*eGFP* reporter and transgenic embryos. The *lhx1* promoters (either wild type or mutant described above) were cloned into the NotI/BamhI sites of *pBS SK I-SceI* (gift of Dr. T. Pieler) to create *lhx1-GFP* and *lhx1*$^{mut\text{-}709}$*-GFP*. Transgenics were generated as previously described (Loeber et al., 2009).

The *Xnr5* promoter was PCR-amplified using primers (*KpnI* adaptor) (ACT AGG TAC CCC TCG GTA ACT TAT CAT ATC) and (*BamHI* adaptor) (CGG GAT CCC GAA GCT TCC AGT GAA TCT T) from *Xenopus laevis* gDNA template isolated from adult *Xenopus laevis* liver to yield a 773bp amplicon (-12 to -785 from ATG) that was ligated into the *pDsRed-express-N1* vector. The *Xnr5:DsRed* transcription cassette was then PCR-amplified using primers (*KpnI* adaptor) (ACT AGG TAC CCC TCG GTA ACT TAT CAT ATC) and (*SacII* adaptor) (TTC CCG CGG GGA CCC TAT CTC GGT CTA TTC) to yield a 1856bp amplicon that was ligated into the *pCS2:HcRed vector*

Xnr5:DsRed/pCS2:HcRed Mutant B Site-directed mutagenesis was used to mutate the putative pitx3 binding site (-228) in the *Xnr5* promoter using primers CAG GTG ACA GGT TC**C Cgg ATC** CTA TGC TAA TAA G and CTT ATT AGC ATA G**GA Tcc GG**G AAC CTG TCA CCT G to introduce a novel *BamHI* site (TAATCC mutated to TA**gg**CC).

Xnr5:DsRed/pCS2:HcRed Mutant C. Site-directed mutagenesis was used to mutate another putative pitx3 binding site (-94) in the *Xnr5* promoter using primers CCT

TAG GAA TGA AG**T cga CT**T CTG AGC ATG ACT and AGT CAT GCT CAG A**AG tcg A**CT TCA TTC CTA AGG to introduce a novel *SalI* site (TAAGCT mutated to TC**gac**T).

All vectors were sequenced for verification of cloning and mutagenesis accuracy. Plasmid DNA was purified using Qiagen Maxi/Midi preparation columns.

Cell cultures. HEK293 cells (kindly gifted by Dr. O. Vacratsis) were cultured in high glucose DMEM (Fisher Scientific) supplemented with 10% fetal bovine serum (Invitrogen) and Penicillin-Streptomycin (500UI and 500ug respectively; Sigma-Aldrich), under standard conditions.

Transient transfections. HEK293 cells were split 24 hours prior to transfection and were 40% confluent at the day of transfection. For the reporter assays, cells grown in 100mm dishes were transfected with 13ug DNA in 750uL DMEM with 25uL 1mg/ml polyethylenimine (PEI; Sigma) (Durocher et al., 2002). A combination of 9ug promoter-reporter vector: 4ug IRES expression vector (later used to express pitx3) was found to be optimal for the flow cytometric detection of both GFP and HcRed transfection control fluors. The DNA/ polyethylenimine transfectant was introduced to cells in plain media, and 4-6 hours post-transfection the serum-free media was replaced with complete media. To the *Tyrosine hydroxylase* experiments 10uM forskolin (LLC Lab) was added after 24 hours and cells were analyzed 48 hours post-transfection. For dilution experiments, various concentrations of expression vector were transfected in combination with titres of pCS2- to yield a total of13ug of DNA for any given transfection. 48 hours post-transfection cells were trypsinized and separated: 2ml were reserved for flow cytometry and 8ml for protein isolation. Time-point experiments were conducted similarly, with

cells transfected with 13ug of DNA and analyzed 24, 36 and 48 hours post-transfection by flow cytometry and Western blotting.

Immunoblotting. Total protein was isolated from cell lysates and 50ug was loaded for SDS-PAGE. Proteins were detected as follows: 32kDa pitx3 1:2000 (ProSci Inc. 1^0 Rabbit Antibody: PAS 3131/3132), 47kDa a-actin 1:10,000 (Sigma 1^0 Rabbit Antibody: A2066), 27kDa eGFP 1:5000 (Torrey Pines Biolabs Inc. 1^0 Rabbit Antibody: TP401), Chemicon International 2^0 Goat Antibody: AQ132P (1:10,000). Protein bands were detected with SuperSignal West Pico Chemiluminescent Substrate (Thermo Scientific) using an Alpha Innotech imager equipped with AlphaEase Fluor Chem HD2 software.

Flow Cytometry. Transfected cells grown for 48 hours in a dark environment were washed with PBS, trypsinized, and re-suspended in the appropriate volume of PBS to conduct flow cytometry utilizing a Beckman Coulter Cytomics FC500 system and the filter/detector system in Table 2 for maximum detection and separation of the three fluors used. Both the uniphase Argon ion and coherent red solid-state diode lasers were enabled. Using CXP software (Beckman Coulter), forward and side scatter enabled the gating of viable single cells. Samples containing each plasmid transfected individually were employed to set gates for the respective fluor, to subtract background fluorescence, and to allow for compensation of their overlapping emission spectra. For each treatment, 10,000 co-transfected cells expressing both GFP and HcRed1 were collected and the total fluorescence intensity for the reporter gene DsRed was calculated. The ratio between fluorescence intensities for the promoter reporter DsRed and its in-vector transfection control gene, HcRed, were related to the fluorescence intensity for GFP (indicative of

transcription factor pitx3) using Weasel software (Walter and Eliza Hall Institute of Medical Research). All experiments were conducted in triplicate.

Channel Detector	Fluorescent Protein	Colour	Excitation Peak (λ max)	Emmision Peak (λ max)	Filter	Voltage	Gain
FL1	eGFP (F64L/S65T)	Green (red-shifted)	490 nm	510nm	525BP	329	1.0
FL2	DsRed	Red-orange	557nm	579nm	575BP	332	1.0
FL5	HcRED	Far-red	588nm	618nm	640LP	500	2.0

Table 2: Flow cytometry system standardization. Different types of optical filters (Band-pass (BP) and long-pass (LP)) are employed to achieve optimal fluor separation.

Statistical analysis. SPSS software was used to assess statistical differences in the total DsRed fluorescence generated in the different conditions of the reporter assay. To determine the effect of pitx3 on a promoter, we used a one-way ANOVA test corroborated with a contrast test to compare the basal levels of the promoter reporter. This was assessed after pitx3 exposure following co-transfection with the wild type or homeodomain binding mutant (BM). For the binding site mutants we employed a T-test to compare the DsRed output of the mutant under basal conditions with the one exposed to pitx3. Tests were considered significant when $p<0.05$.

RNA in situ hybridizations were performed essentially as previously described (Harland, 1991)

Acknowledgements

This work was supported by Natural Sciences and Engineering Research Discovery Grant 203459 to MJC and 05947 to JWH. Thanks are due to Kristi Thompson of the Leddy Library Academic Data Centre, and to Chantal Dings-Avery for help and advice on statistical analysis.

References

Amendt BA, Sutherland LB, Russo AF. 1999. Multifunctional role of the Pitx2 homeodomain protein C-terminal tail. Mol Cell Biol 19:7001-7010.

Artinger M, Blitz I, Inoue K, Tran U, Cho KW. 1997. Interaction of goosecoid and brachyury in Xenopus mesoderm patterning. Mech Dev 65:187-196.

Beachy PA, Krasnow MA, Gavis ER, Hogness DS. 1988. An Ultrabithorax protein binds sequences near its own and the Antennapedia P1 promoters. Cell 55:1069-1081.

Cazorla P, Smidt MP, O'Malley KL, Burbach JP. 2000. A response element for the homeodomain transcription factor Ptx3 in the tyrosine hydroxylase gene promoter. J Neurochem 74:1829-1837.

Cha YR, Takahashi S, Wright CV. 2006. Cooperative non-cell and cell autonomous regulation of Nodal gene expression and signaling by Lefty/Antivin and Brachyury in Xenopus. Dev Biol 290:246-264.

Cirio MC, Hui Z, Haldin CE, Cosentino CC, Stuckenholz C, Chen X, Hong SK, Dawid IB, Hukriede NA. 2011. Lhx1 is required for specification of the renal progenitor cell field. PLoS One 6:e18858.

Conlon FL, Sedgwick SG, Weston KM, Smith JC. 1996. Inhibition of Xbra transcription activation causes defects in mesodermal patterning and reveals autoregulation of Xbra in dorsal mesoderm. Development 122:2427-2435.

Coulon V, L'Honore A, Ouimette JF, Dumontier E, van den Munckhof P, Drouin J. 2007. A muscle-specific promoter directs Pitx3 gene expression in skeletal muscle cells. J Biol Chem 282:33192-33200.

Durocher Y, Perret S, Kamen A. 2002. High-level and high-throughput recombinant protein production by transient transfection of suspension-growing human 293-EBNA1 cells. Nucleic Acids Res 30:E9.

Dutta S, Dietrich JE, Aspock G, Burdine RD, Schier A, Westerfield M, Varga ZM. 2005. pitx3 defines an equivalence domain for lens and anterior pituitary placode. Development 132:1579-1590.

Fossat N, Ip CK, Jones VJ, Studdert JB, Khoo PL, Lewis SL, Power M, Tourle K, Loebel DA, Kwan KM, Behringer RR, Tam PP. 2015. Context-specific function of the LIM homeobox 1 transcription factor in head formation of the mouse embryo. Development 142:2069-2079.

Harland RM. 1991. In situ hybridization: an improved whole-mount method for *Xenopus* embryos. Methods Cell Biol 36:685-695.

Hooker L, Smoczer C, Khosrowshahian F, Wolanski M, Crawford MJ. 2012. Microarray based identification of Pitx3 targets during Xenopus embryogenesis. Dev Dyn.

Hukriede NA, Tsang TE, Habas R, Khoo PL, Steiner K, Weeks DL, Tam PP, Dawid IB. 2003. Conserved requirement of Lim1 function for cell movements during gastrulation. Dev Cell 4:83-94.

Inoue J, Ueda Y, Bando T, Mito T, Noji S, Ohuchi H. 2013. The expression of LIM-homeobox genes, Lhx1 and Lhx5, in the forebrain is essential for neural retina differentiation. Dev Growth Differ 55:668-675.

Kawaue T, Okamoto M, Matsuyo A, Inoue J, Ueda Y, Tomonari S, Noji S, Ohuchi H. 2012. Lhx1 in the proximal region of the optic vesicle permits neural retina development in the chicken. Biol Open 1:1083-1093.

Khosrowshahian F, Wolanski M, Chang WY, Fujiki K, Jacobs L, Crawford MJ. 2005. Lens and retina formation require expression of Pitx3 in Xenopus pre-lens ectoderm. Dev Dyn 234:577-589.

Kim SH, Jen WC, De Robertis EM, Kintner C. 2000. The protocadherin PAPC establishes segmental boundaries during somitogenesis in xenopus embryos. Curr Biol 10:821-830.

L'Honore A, Coulon V, Marcil A, Lebel M, Lafrance-Vanasse J, Gage P, Camper S, Drouin J. 2007. Sequential expression and redundancy of Pitx2 and Pitx3 genes during muscle development. Dev Biol 307:421-433.

Lebel M, Gauthier Y, Moreau A, Drouin J. 2001. Pitx3 activates mouse tyrosine hydroxylase promoter via a high-affinity binding site. J Neurochem 77:558-567.

Loeber J, Pan FC, Pieler T. 2009. Generation of transgenic frogs. Methods Mol Biol 561:65-72.

Luxardi G, Marchal L, Thome V, Kodjabachian L. 2010. Distinct Xenopus Nodal ligands sequentially induce mesendoderm and control gastrulation movements in parallel to the Wnt/PCP pathway. Development 137:417-426.

Mangold O. 1933. Uber die induktionsfahigkeit der verschiedenen Bezirke der Neurula von Urodelen. Naturwissenschaften 43:761-766.

Maxwell SL, Ho HY, Kuehner E, Zhao S, Li M. 2005. Pitx3 regulates tyrosine hydroxylase expression in the substantia nigra and identifies a subgroup of mesencephalic dopaminergic progenitor neurons during mouse development. Dev Biol 282:467-479.

Mead PE, Brivanlou IH, Kelley CM, Zon LI. 1996. BMP-4-responsive regulation of dorsal-ventral patterning by the homeobox protein Mix.1. Nature 382:357-360.

Medina-Martinez O, Shah R, Jamrich M. 2009. Pitx3 controls multiple aspects of lens development. Dev Dyn 238:2193-2201.

Messmer K, Remington MP, Skidmore F, Fishman PS. 2007. Induction of tyrosine hydroxylase expression by the transcription factor Pitx3. Int J Dev Neurosci 25:29-37.

Mochizuki T, Karavanov AA, Curtiss PE, Ault KT, Sugimoto N, Watabe T, Shiokawa K, Jamrich M, Cho KW, Dawid IB, Taira M. 2000. Xlim-1 and LIM domain binding protein 1 cooperate with various transcription factors in the regulation of the goosecoid promoter. Dev Biol 224:470-485.

Ohi Y, Wright CV. 2007. Anteriorward shifting of asymmetric Xnr1 expression and contralateral communication in left-right specification in Xenopus. Dev Biol 301:447-463.

Onuma Y, Takahashi S, Haramoto Y, Tanegashima K, Yokota C, Whitman M, Asashima M. 2005. Xnr2 and Xnr5 unprocessed proteins inhibit Wnt signaling upstream of dishevelled. Dev Dyn 234:900-910.

Ovcharenko I, Loots GG, Giardine BM, Hou M, Ma J, Hardison RC, Stubbs L, Miller W. 2005. Mulan: multiple-sequence local alignment and visualization for studying function and evolution. Genome Res 15:184-194.

Pommereit D, Pieler T, Hollemann T. 2001. *Xpitx3*: a member of the *Rieg/Pitx* gene family expressed during pituitary and lens formation in *Xenopus laevis*. Mech Dev 102:255-257.

Reddy SD, Rayala SK, Ohshiro K, Pakala SB, Kobori N, Dash P, Yun S, Qin J, O'Malley

BW, Kumar R. 2011. Multiple coregulatory control of tyrosine hydroxylase gene transcription. Proc Natl Acad Sci U S A 108:4200-4205.

Sakuma R, Ohnishi Yi Y, Meno C, Fujii H, Juan H, Takeuchi J, Ogura T, Li E, Miyazono K, Hamada H. 2002. Inhibition of Nodal signalling by Lefty mediated through interaction with common receptors and efficient diffusion. Genes Cells 7:401-412.

Semina EV, Ferrell RE, Mintz-Hittner HA, Bitoun P, Alward WL, Reiter RS, Funkhauser C, Daack-Hirsch S, Murray JC. 1998. A novel homeobox gene PITX3 is mutated in families with autosomal-dominant cataracts and ASMD. Nat Genet 19:167-170.

Shawlot W, Behringer RR. 1995. Requirement for Lim1 in head-organizer function. Nature 374:425-430.

Smidt MP, Smits SM, Burbach JP. 2004. Homeobox gene Pitx3 and its role in the development of dopamine neurons of the substantia nigra. Cell Tissue Res 318:35-43.

Smidt MP, van Schaick HS, Lanctot C, Tremblay JJ, Cox JJ, van der Kleij AA, Wolterink G, Drouin J, Burbach JP. 1997. A homeodomain gene Ptx3 has highly restricted brain expression in mesencephalic dopaminergic neurons. Proc Natl Acad Sci U S A 94:13305-13310.

Smith JC, Price BM, Green JB, Weigel D, Herrmann BG. 1991. Expression of a Xenopus homolog of Brachyury (T) is an immediate-early response to mesoderm induction. Cell 67:79-87.

Smoczer C, Hooker L, Brode S, Wolanski M, KhosrowShahian F, Crawford M. 2013. The Xenopus homeobox gene pitx3 impinges upon somitogenesis and laterality. Biochem Cell Biol 91:79-87.

Stables J, Scott S, Brown S, Roelant C, Burns D, Lee MG, Rees S. 1999. Development of a dual glow-signal firefly and Renilla luciferase assay reagent for the analysis of G-protein coupled receptor signalling. J Recept Signal Transduct Res 19:395-410.

Tadjuidje E, Kofron M, Mir A, Wylie C, Heasman J, Cha SW. 2016. Nodal signalling in Xenopus: the role of Xnr5 in left/right asymmetry and heart development. Open Biol 6.

Taira M, Jamrich M, Good PJ, Dawid IB. 1992. The LIM domain-containing homeo box gene Xlim-1 is expressed specifically in the organizer region of Xenopus gastrula embryos. Genes Dev 6:356-366.

Takahashi S, Yokota C, Takano K, Tanegashima K, Onuma Y, Goto J, Asashima M. 2000. Two novel nodal-related genes initiate early inductive events in Xenopus Nieuwkoop center. Development 127:5319-5329.

Trouet D, Nilius B, Voets T, Droogmans G, Eggermont J. 1997. Use of a bicistronic GFP-expression vector to characterise ion channels after transfection in mammalian cells. Pflugers Arch 434:632-638.

Uhlen M, Fagerberg L, Hallstrom BM, Lindskog C, Oksvold P, Mardinoglu A, Sivertsson A, Kampf C, Sjostedt E, Asplund A, Olsson I, Edlund K, Lundberg E, Navani S, Szigyarto CA, Odeberg J, Djureinovic D, Takanen JO, Hober S, Alm T, Edqvist PH, Berling H, Tegel H, Mulder J, Rockberg J, Nilsson P, Schwenk JM, Hamsten M, von Feilitzen K, Forsberg M, Persson L, Johansson F, Zwahlen M, von Heijne G, Nielsen J, Ponten F. 2015. Proteomics. Tissue-based map of the

human proteome. Science 347:1260419.
van den Munckhof P, Luk KC, Ste-Marie L, Montgomery J, Blanchet PJ, Sadikot AF, Drouin J. 2003. Pitx3 is required for motor activity and for survival of a subset of midbrain dopaminergic neurons. Development 130:2535-2542.
Volpicelli F, De Gregorio R, Pulcrano S, Perrone-Capano C, di Porzio U, Bellenchi GC. 2012. Direct regulation of Pitx3 expression by Nurr1 in culture and in developing mouse midbrain. PLoS One 7:e30661.

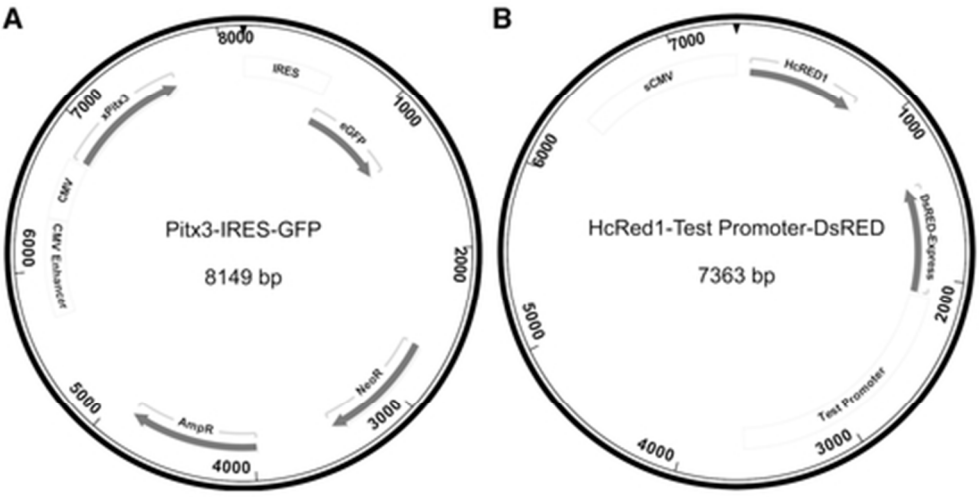

General structure of expression and reporter plasmids. (A) Expression plasmid with ORF of pitx3 bicistronically linked to eGFP. (B) Reporter plasmid with the reporter gene DsRed-express driven by the tested promoter, cloned in opposite orientation from the transfection control gene HcRed1 driven constitutively by CMV.

43x22mm (300 x 300 DPI)

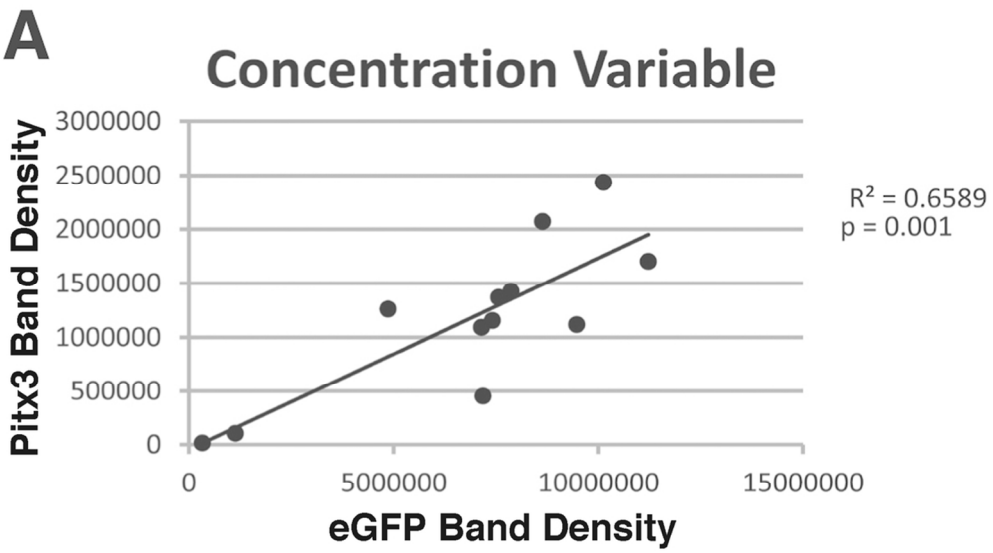

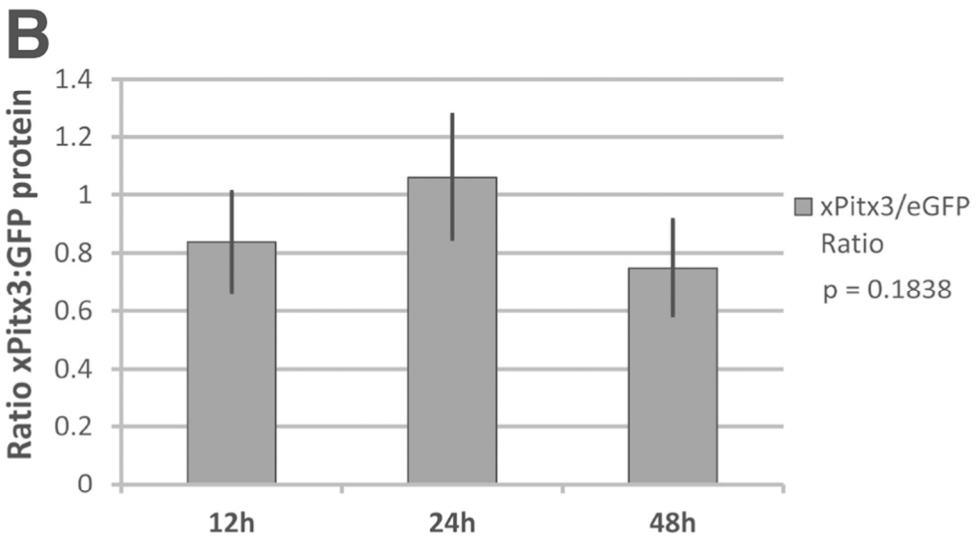

Correlation between the pitx3 and GFP proteins. The proteins were assayed by Western blotting and the amount of each protein was assessed as the optical integrated density value of the respective band. (A) Regression analysis to correlate the levels of pitx3 and GFP proteins in cells transfected with different concentrations of expression vector. (B) Ratios between the levels of pitx3 and GFP protein in cells transfected with a set concentration of expression vector and analyzed at 24, 36 and 48 hours post-transfection. There is no statistically significant difference between time points of this range.

101x121mm (300 x 300 DPI)

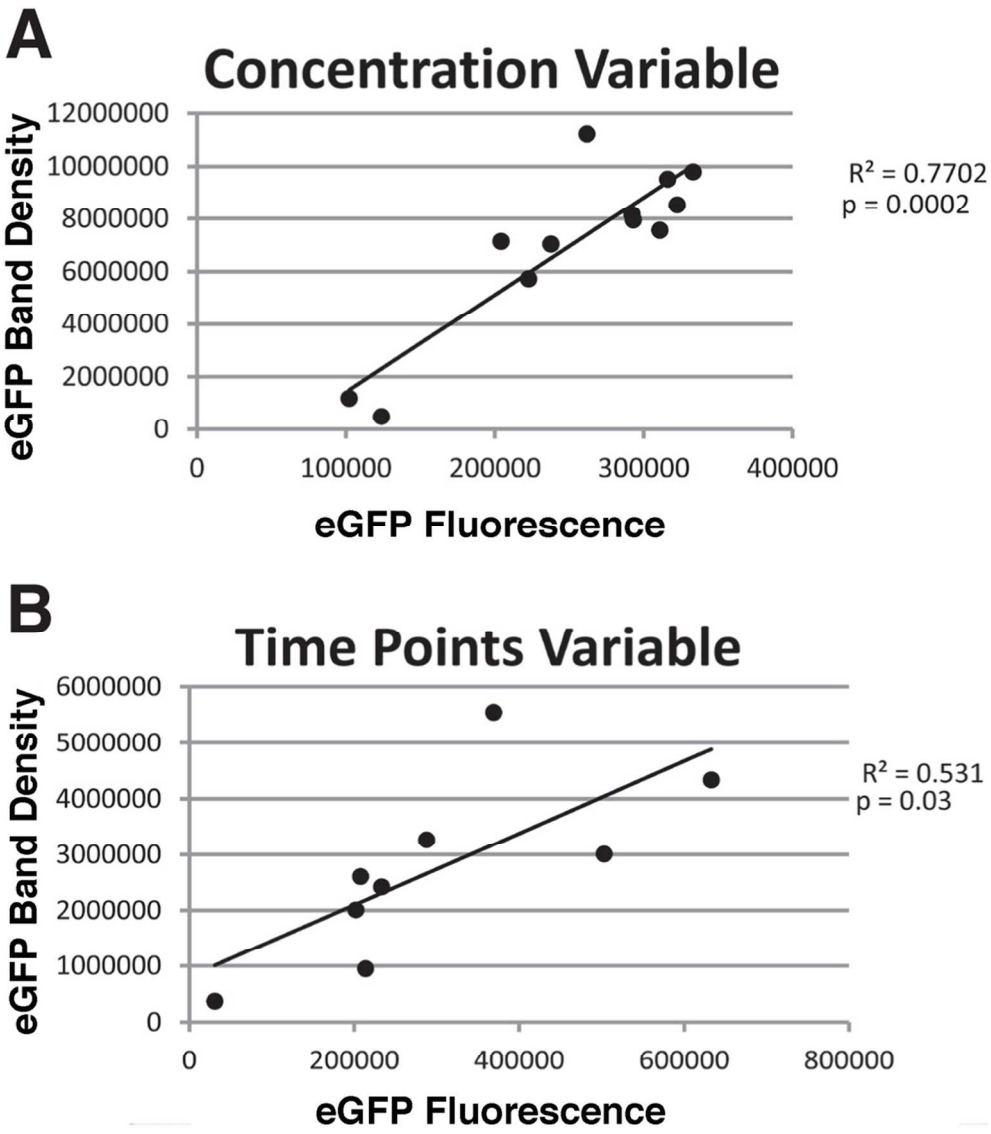

Correlation between GFP protein and GFP fluorescence. The GFP protein levels were determined by Western blotting and evaluated as the optical density of the band on the blot. A percentage of the total cells were used to detect the fluorescence using flow cytometry. (A) Regression analysis to correlate GFP protein levels and GFP fluorescence in cells transfected with 4 decreasing concentrations of expression vector by 1.3 fold. (B) Linear regression between the GFP protein and fluorescence in cells transfected with equal concentrations of expression vector and evaluated at 3 different times post-transfection.

98x114mm (300 x 300 DPI)

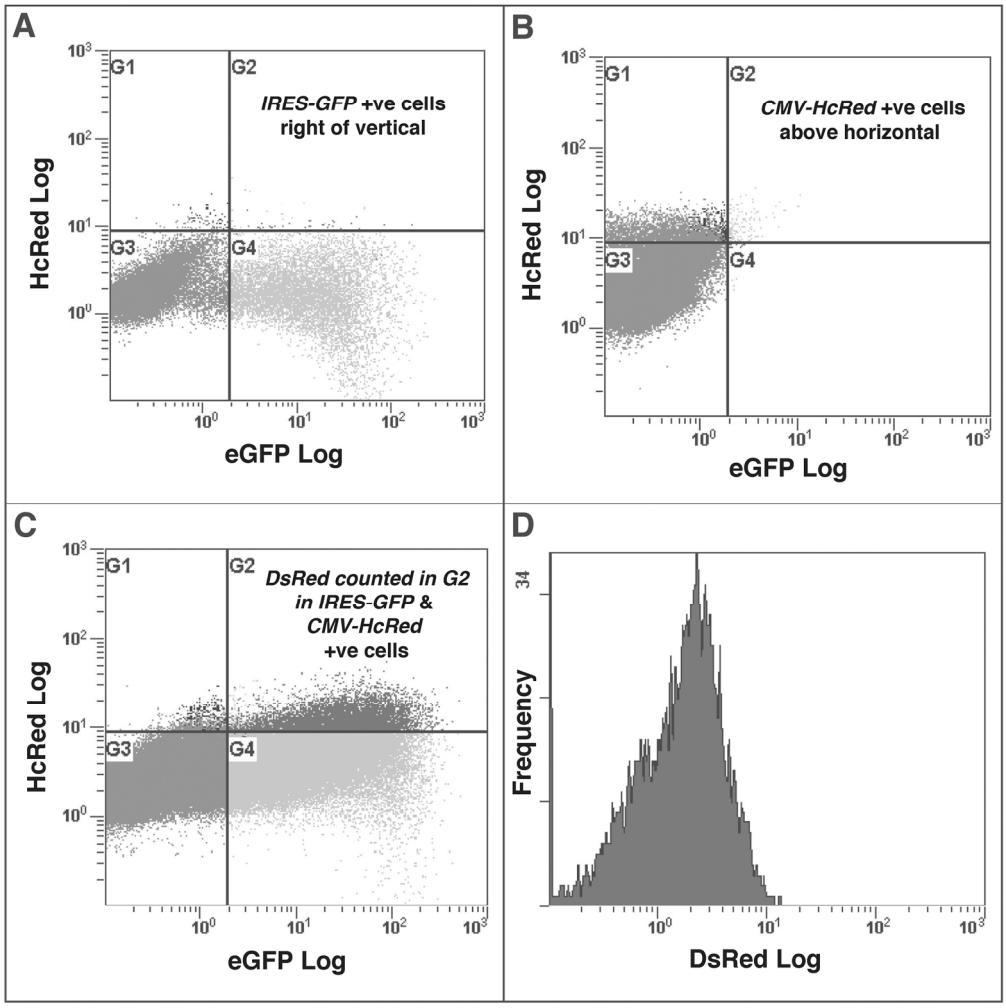

Figure 4: Flow cytometer set-up to detect the three fluors in the new reporter assay. (A) Gate set-up was arranged to minimize spectral overlap and background. For eGFP in FL1 for cells transfected with the IRES-GFP control vector relegates GFP counts to the right of the vertical line in quadrant G4. (B) Cells transfected with CMV-HcRed control plasmid, recorded in FL5 and gated for HcRed1 expression relegates HcRed counts to above the horizontal line in quadrant G1. (C) Gated population of 10,000 cells expressing eGFP, HcRed1, and DsRed (Ds Red, indicative of promoter activity is counted in quadrant G2). (D) Histogram of DsRed output in FL2 for the population of eGFP and HcRed co-expressing cells.

174x174mm (300 x 300 DPI)

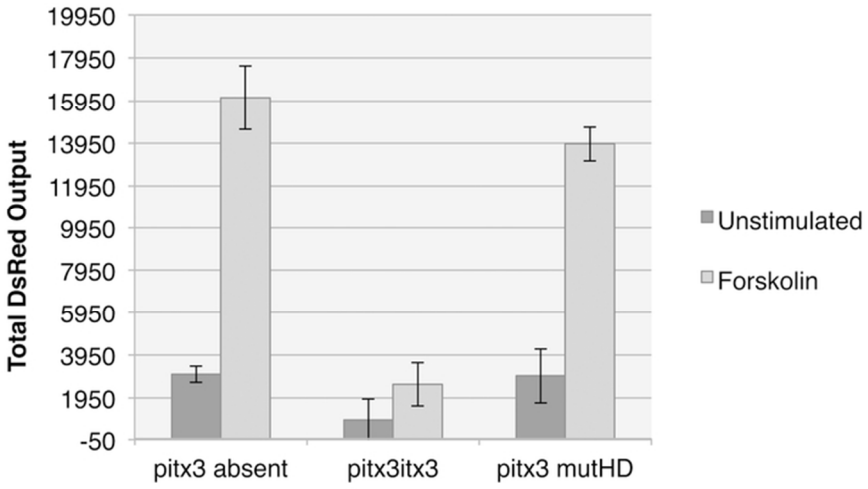

Combination		Statistical Significance (Post Hoc Tukey)				
pitx3 absent	Th promoter	.000	ns	ns	ns	.001
	Th prom + F	-	.000	.000	.001	ns
pitx3 protein	Th promoter		-	ns	ns	.000
	Th prom + F			-	ns	.001
pitx3^{mutHD}	Th promoter				-	.002
	Th prom + F					-

Combination	Th prom+ F	Th promoter	Th prom + F	Th promoter	Th prom + F
	pitx3 absent	pitx3 protein		pitx3^{mutHD}	

Pitx3 represses the Th (tyrosine hydroxylase) promoter. The Th reporter (plasmid CMV-HcRed/Th-DsRed) was tested, under conditions of presence or absence of forskolin, to see how it responded to vectors for pitx3 absent (IRES-GFP), pitx3 protein (pitx3-IRES-GFP), or pitx3 mutHD expressing a homeodomain mutant (pitx3mutHD-IRES-GFP). ANOVA demonstrated that statistically significant differences existed,. A post-hoc Tukey test determined specifically which comparisons were significant and p values are reported above. ns – denotes no significant difference.

69x57mm (300 x 300 DPI)

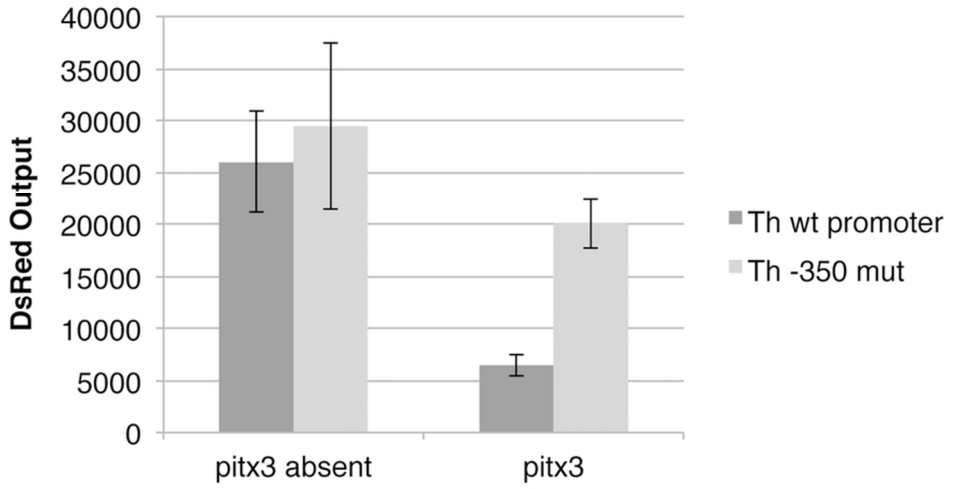

Combination		Statistical Significance (Post Hoc Tukey)		
pitx3 absent	Th promoter	ns	.005	ns
	Th -350 mut	-	.002	ns
pitx3	Th promoter		-	.037
	Th -350 mut			-
Combination		Th -350 mut	Th promoter	Th -350 mut
		pitx3 absent	pitx3	

The Th (Tyrosine hydroxylase) promoter binding motif for pitx3 is important for repression. Wildtype and mutant Th reporters (wt - CMV-HcRed/Th-DsRed; mutant - CMV-HcRed/Thmut-350-DsRed) were tested under conditions of the presence or absence of pitx3 (absent - plasmid IRES-GFP; pitx3 present – plasmid pitx3-IRES-GFP). ANOVA demonstrated that statistically significant differences existed. A post-hoc Tukey test determined specifically which comparisons were significant and p values are reported above. ns – denotes no significant difference.

80x75mm (300 x 300 DPI)

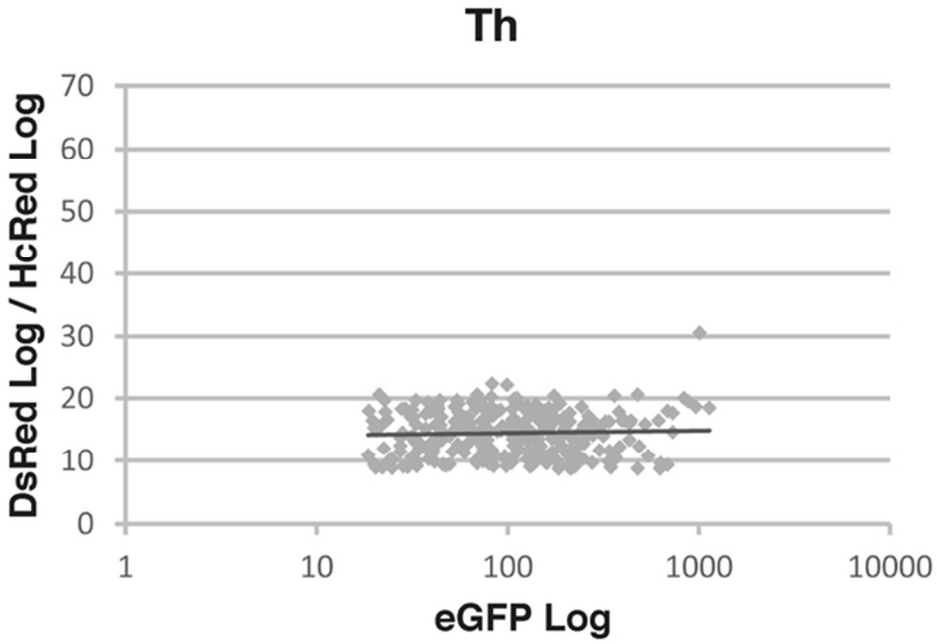

Th promoter is activated in linear fashion by pitx3. Transcription factor activity was assessed in cells expressing all three fluors, by plotting the normalized DsRed output to the GFP input and determining the generated trend line.

58x39mm (300 x 300 DPI)

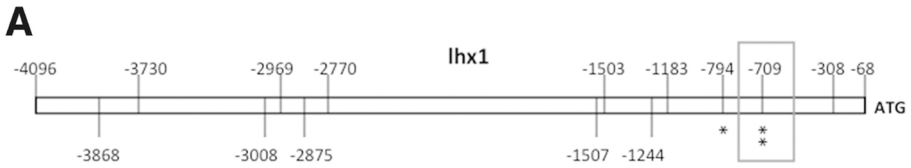

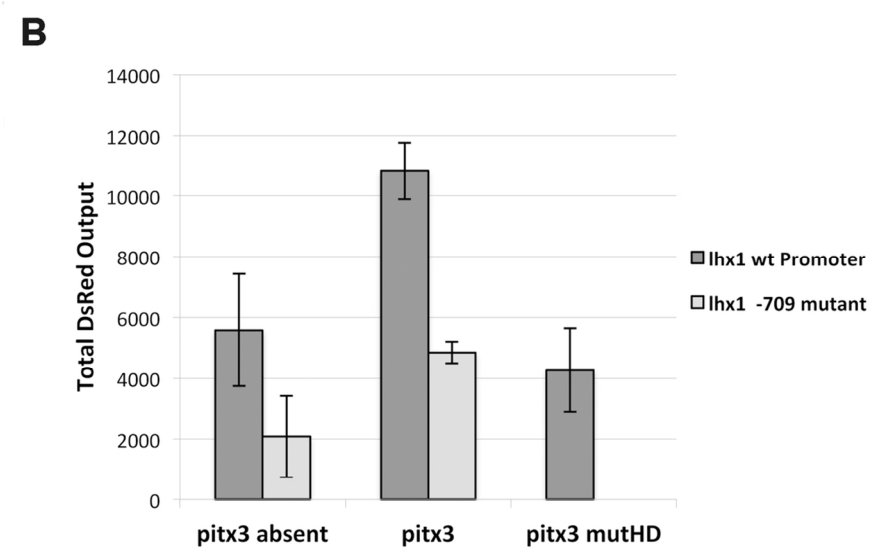

Combination		Statistical Significance (Post-Hoc Tukey)			
pitx3 absent	lhx1 promoter	.044	.004	ns	ns
	lhx1 mutant$^{mut-709}$	-	.000	ns	ns
pitx3 protein	lhx1 promoter		-	.001	.001
	lhx1 mutant$^{mut-709}$			-	ns
pitx3^{mutHD}	lhx1 promoter				-
Combination		lhx1$^{mut-709}$	lhx1 promoter	lhx1$^{mut-709}$	lhx1 promoter
		pitx3 absent	pitx3 protein		pitx3^{mutHD}

lhx1 promoter activation by pitx3. Vectors for pitx3 absent (IRES-GFP), pitx3 protein (pitx3-IRES-GFP), or pitx3 mutHD expressing a homeodomain mutant (pitx3mutHD-IRES-GFP) were tested for their ability to activate a wildtype lhx1wt promoter-driven DsRed reporter (CMV-HcRed/lhx1-DsRed), and a pitx3 binding motif mutant lhx11mut-709 promoter-driven DsRed reporter (CMV-HcRed/lhx1mut-709-DsRed). ANOVA demonstrated that statistically significant differences existed. A post-hoc Tukey test determined specifically which comparisons were significant and p values are reported above. ns – denotes no significant difference.

107x136mm (300 x 300 DPI)

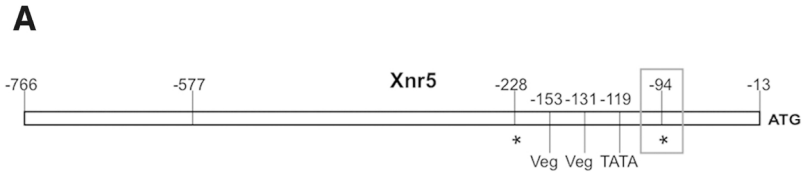

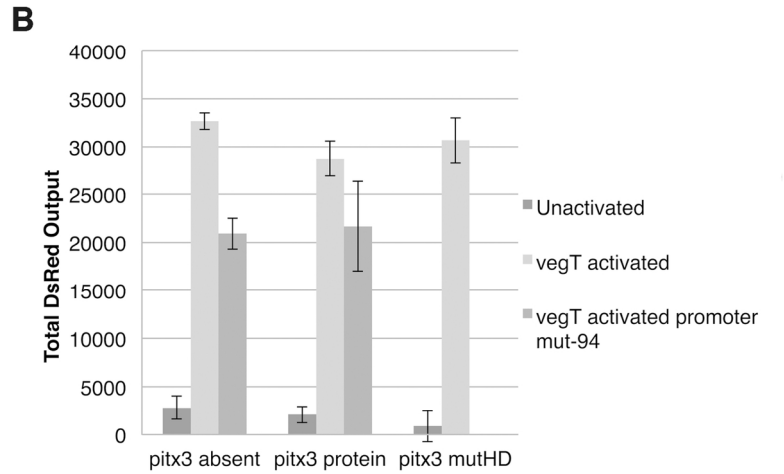

Combination		Statistical Significance (Post Hoc Tukey)						
pitx3 absent	not activated	.000	.000	ns	.000	.000	ns	.000
	vegT	-	.000	.000	ns	.000	.000	ns
	vegT promoter mut-94		-	.000	.01	ns	.000	.001
pitx3	not activated			-	.000	.000	ns	.000
	vegT				-	.023	.000	ns
	vegT promoter mut-94					-	.000	.003
pitx3 mutHD	not activated						-	.000
	vegT							-
Combination		vegT	vegT promoter mut-94	not activated	vegT	vegT promoter mut-94	not activated	vegT
		pitx3 absent		pitx3			pitx3 mutHD	

The xnr5 promoter is repressed by pitx3. Wildtype and mutant xnr5 reporters (wt - CMV-HcRed/xnr5-DsRed; mutant - CMV-HcRed/xnr5mut-3-94-DsRed) were tested under conditions of the presence or absence of pitx3 (absent - plasmid IRES-GFP; pitx3 present – plasmid pitx3-IRES-GFP), as well as in the presence or absence of an activator, vegT, or a pitx3 homeodomain mutant pitx3mutHD-IRES-GFP. ANOVA demonstrated that statistically significant differences existed. A post-hoc Tukey test determined specifically which comparisons were significant and p values are reported above. ns – denotes no significant difference.

125x186mm (300 x 300 DPI)

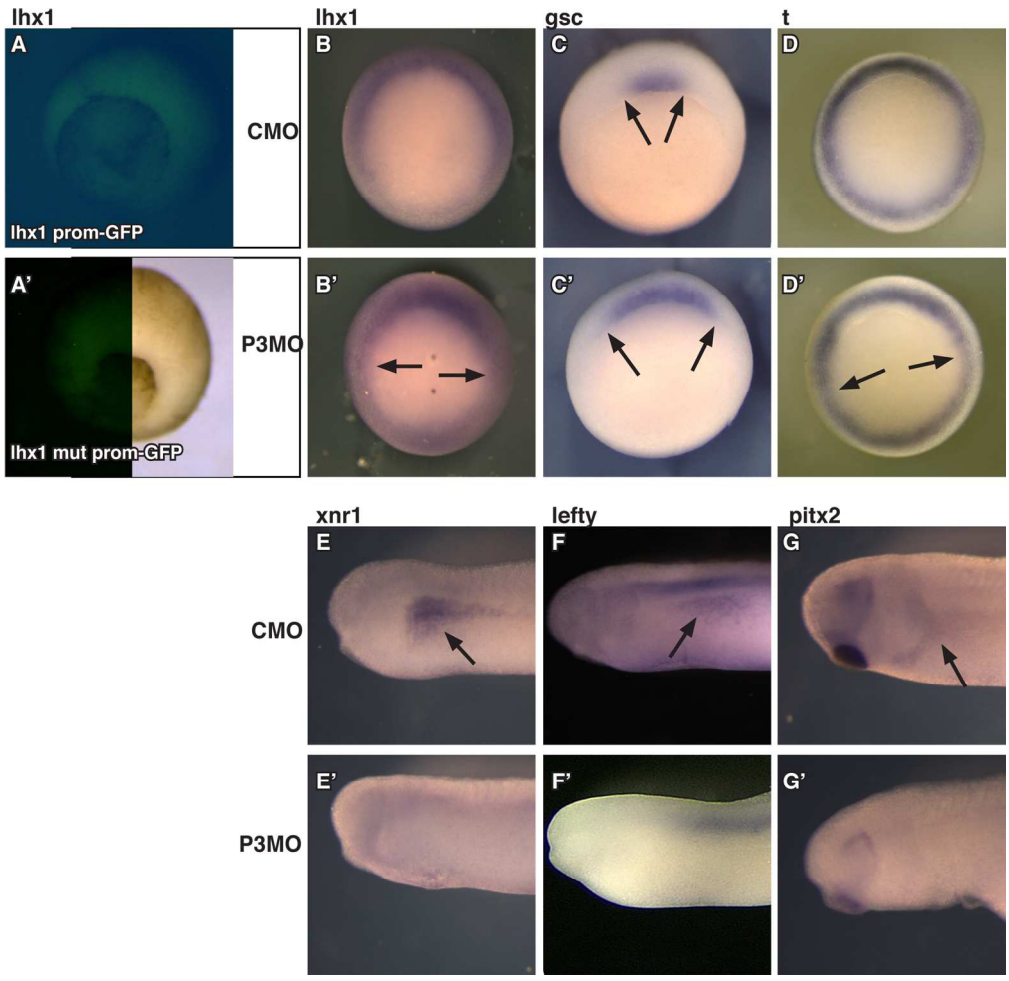

Differential gene expression at early gastrula stages and during laterality. (A, A') A GFP reporter expresses when the pitx3 binding site in the lhx1 promoter is intact (A), but is down-regulated when mutated (split exposure image in A'; both fluorescence images exposed 19 seconds). (B-D) Vegetal view of embryos injected with control-morpholino (CMO) display wildtype gene expression patterns. (B'-D'), but pitx3-morpholino (P3MO) affects gene expression during the beginning of gastrulation. Dorsal lip is oriented to the top. Note the lateral depression of lateral lhx1 and t (arrows in B' and D' respectively) and expansion of gsc expression in P3MO embryos knockdown embryos (compare C and C' arrows). (E-G) Genes participating in the laterality signal cascade are normally expressed in left lateral plate mesoderm (arrows). (E'-G') In morphants where pitx3 is knocked down, expression of xnr5 downstream targets xnr1, lefty and pitx2 is decreased or absent in the left lateral plate mesoderm (arrows).

175x169mm (300 x 300 DPI)